# B cell-intrinsic function of TAPP adaptors in controlling germinal center responses and autoantibody production in mice

Jayachandran, Nipun; Landego, Ivan; Hou, Sen; Alessi, Dario; Marshall, Aaron J.

*Published in:*
European Journal of Immunology

*DOI:*
10.1002/eji.201646596

*Publication date:*
2017

*Document Version*
Peer reviewed version

# B cell-intrinsic function of TAPP adaptors in controlling germinal center responses and autoantibody production in mice

Nipun Jayachandran[1], Ivan Landego[1], Sen Hou[1], Dario R. Alessi[2] and Aaron J. Marshall[1,3]

[1] Department of Immunology, University of Manitoba, 471 Apotex Centre, 750 McDermot Avenue, Winnipeg, MB, Canada R3E-0T5

[2] College of Life Sciences, University of Dundee, Dundee DD1 5EH, Scotland, United Kingdom

[3] Corresponding author: aaron.marshall@umanitoba.ca; Ph 204 789-3385; Fax 789-3921

**Key words:** Antibodies, Autoimmunity, B cells, Cellular activation, Signal transduction

**Abbreviations:** TAPP: Tandem PH domain containing Proteins, GC: Germinal center, BCR: B cell antigen receptor, TFH: T follicular helper cell, GCB: Germinal center B cell, BM: Bone marrow.

## Abstract

Control of B-cell signal transduction is critical to prevent production of pathological autoantibodies. Tandem PH domain containing proteins (TAPPs) specifically bind PI(3,4)P2, a phosphoinositide product generated by PI 3-kinases and the phosphatase SHIP. TAPP KI mice bearing PH domain-inactivating mutations in both TAPP1 and TAPP2 genes, uncoupling them from PI(3,4)P2, exhibit increased BCR-induced activation of the kinase Akt and develop lupus-like characteristics including anti-DNA antibodies and deposition of immune complexes in kidneys. Here we find that TAPP KI mice develop chronic germinal centers (GCs) with age and show abnormal expression of B cell activation and memory markers. Upon immunization with T-dependent Ag, TAPP KI mice develop functional but abnormally large GCs, associated with increased GC B cell survival. Disruption of chronic GCs in TAPP KI mice by deletion of the costimulatory molecule ICOS abrogate anti-DNA and anti-nuclear antibody production in TAPP KI mice, indicating an essential role for GCs. Moreover, TAPP KI B cells are sufficient to drive chronic GC responses and recapitulate the autoimmune phenotype in bone marrow chimeric mice. Our findings demonstrate a B cell-intrinsic role of TAPP-PI(3,4)P2 interaction in regulating GC responses and autoantibody production and suggest that uncontrolled Akt activity in B cells can drive autoimmunity.

## Introduction

Phosphoinositide 3-kinases (PI3K) play critical roles in B cell activation via their antigen receptor (BCR) and other key receptors [1-3]. Class I PI3Ks mediate downstream signaling by phosphorylating plasma membrane lipids to generate the phosphoinositide second messengers PI(3,4,5)P3 and PI(3,4)P2. The dynamics of these lipid second messengers are tightly regulated by PI phosphatases PTEN, INPP4 and SHIP which dephosphorylate the 3, 4 or 5 position of the PI headgroup, respectively [4, 5]. PI phosphatases, together with PI3Ks, can thus control the plasma membrane localization and function of specific PI-binding signaling proteins that collectively determine the downstream response. PI3K plays an essential role in maintaining mature B cell survival, which depends on tonic BCR signaling [6, 7]. In B cell malignancies that depend on aberrant chronic BCR signaling, blockade of PI3K signaling has been found to be an effective therapeutic strategy [1, 8].

Dysregulation of the PI3K pathway has been associated with lupus-like autoimmune disease in mouse models and in humans. SHIP-/- mice exhibited B cell hyper-responsiveness, splenomegaly and abnormally elevated antibody production [9, 10]. SHIP was found to be activated in anergic B cells and B cell-specific deletion of SHIP resulted in development of lupus-like phenotype [11]. B cell-specific deletion of SHIP also resulted in failure to develop tolerance to artificial autoantigens in BCR transgenic models [11, 12]. The inhibitory receptor FcγRIIB functions in part through activation of SHIP [13], and polymorphisms in *fcgr2b* have been linked to lupus in mouse models and humans [14-16]. Thus, regulation of phosphoinositide accumulation is critical for control of autoreactive B cells and failure to properly control the PI3K pathway can contribute to development of autoimmunity.

B cell proliferation and death in germinal centers (GC) is critical for generation of both protective antibodies and pathogenic autoantibodies. Selective survival and expansion of B cells capable of producing mutated, high affinity antibody depends on both BCR signaling and Ag presentation to follicular helper T cells (Tfh). The PI3K pathway is known to critical roles in both GC B cell and Tfh functions [17]. Genetic disruption of the p110δ PI3K leads to a virtual absence of GCs [18, 19]. The PI3K pathway appears to be highly active within GC B cells based on high levels of phosphorylation of the PI3K-dependent kinase Akt [20], which may be important to maintain survival of GC B cells by promoting expression of BCL-2 family member Mcl-1 [21]. p110δ PI3K also plays a role in induction of the key GCB transcriptional regulator BCL6 [22] and can modulate expression of the enzyme AID [23] which drives antibody diversification within GC.

Phosphoinositides mediate their cellular functions by binding to effector proteins containing PI-binding modules such as PH domains [24, 25]. Well-characterized PI binding proteins functioning in B cell activation include the protein kinases Akt and Btk, which have distinct specificity in binding PI species. Akt binds with similar affinity to the SHIP substrate PI(3,4,5)P3 and its product PI(3,4)P2 [26], while Btk exclusively binds PI(3,4,5)P3 [27]. PI(3,4)P2 binding can activate Akt activity in vitro [26, 28]; however its function in vivo remains unclear. Tandem PH domain containing adaptor proteins 1 and 2 (TAPP1 and TAPP2) are the best characterized proteins that specifically interact with the product of SHIP PI(3,4)P2, but not its substrate PI(3,4,5)P2 [29, 30]. Co-engagement of BCR and FcγRIIB enhances activation of SHIP, leading to more conversion of PI(3,4,5)P3 to PI(3,4)P2 [31-33]. Thus SHIP can function to inhibit membrane recruitment of PI(3,4,5)P3-binding proteins such as Btk, but can also enhance recruitment of PI(3,4)P2-binding proteins such as TAPP1&2 [33].

TAPP adaptors contain a unique and well-characterized phosphoinositide binding pocket in their C-terminal PH domain [29], which has enabled introduction of mutations that specifically disrupt PI(3,4)P2 binding [34]. Mice bearing inactivating mutations in the C-terminal PH domains of both TAPP1 and TAPP2 (TAPP KI) were found to develop lupus-like characteristics including generation of anti-DNA and anti-nuclear antibodies [35]. In this study, we have explored the mechanisms underlying autoimmunity in TAPP KI mice. We find that uncoupling TAPPs from PI(3,4)P2 in B cells leads to abnormal germinal centre responses which are critical for driving autoantibody production. These findings implicate TAPPs as important regulators of the germinal center response which control autoreactive B cells via binding to the phosphoinositide product of SHIP.

## Results

### Abrogation of TAPP - PI (3,4)P2 interaction results in spontaneous B cell activation and chronic GCs

We previously found that mice bearing inactivating mutations in the PI(3,4)P2-binding PH domains of TAPP1 and TAPP2 (TAPP KI) develop a lupus-like autoimmune disease manifesting as autoantibody production detectable by 20 weeks of age [35]. To investigate the basis for this autoimmune pathology we assessed whether middle aged TAPP KI mice display any abnormalities in their B cell populations. At 28-30 weeks of age, TAPP KI splenic B cells exhibited increased frequencies of cells expressing germinal centre B cell (GCB) markers GL7 and Fas (Figure 1A and Supplementary Figure 1). This elevated frequency of GCB was associated with a proportional increase in the $PD1^+$ $ICOS^+$ T follicular helper (Tfh) cell population (Figure 1B). Flow cytometry gating of GCB and Tfh populations was controlled using age-matched mice genetically deficient in p110δ PI3K activity, which lack these populations [17, 19]. Middle-aged TAPP KI mice also showed a significant increase of $CD80^+$ B cells in the spleen and a trend toward elevated CD86 expression (Figure 1C and Supplementary Figure 2). Similar increases in GCB and $CD80^+$ B cells were observed in mesenteric lymph nodes of TAPP KI mice (Figure 1D). Together these results demonstrate that TAPP KI mice develop B cell hyper-activation and chronic GC formation.

### Development of chronic GC in TAPP KI mice is age and gene dose dependent

Abnormal chronic GCs have been associated with autoimmunity in mice as well as humans [36, 37]; thus we further examined the kinetics and gene dose dependence of chronic GC development in the TAPP KI model. Increased GCB and Tfh populations were detectable by 12 weeks of age and increased over time (Figure 2A/B). Frequencies of GCB and Tfh cells were found to be highly

sensitive to WT TAPP gene dosage, with heterozygote mice bearing a single normal TAPP1 and TAPP2 allele showing GCB and Tfh frequencies similar to controls (Figure 2C/D). The frequencies of $CD80^+$ splenic B cells also showed progressive increase with age (Figure 2E) and a similar dependence on WT TAPP gene dosage (Figure 2F), suggesting that generation of this B cell population may be related to the chronic GC response.

**Uncoupling of TAPP adaptors from PI(3,4)P2 results in abnormal GC responses upon immunization**

To assess the impact of TAPP–PI(3,4)P2 interaction on the GC response induced by immunization, 8-10 week old TAPP KI mice were immunized with T dependent antigens NP-OVA/alum or sheep red blood cells. Flow cytometry analyses revealed that approximately 2 fold increases in the frequency of GC B cells in immunized TAPP KI mice (Figure 3A). Immunofluorescence staining of spleen sections showed that TAPP KI GCs show no obvious abnormality in structure or positioning near the interface of B and T cell zones (Figure 3B and Supplementary Figure 3) but have a larger average area. Follicular helper T cell frequencies were correspondingly increased in immunized TAPP KI mice (Figure 3C), however the GCB:Tfh ratio was not significantly different from controls. TAPP KI mice show no significant difference in generation of high affinity anti-NP Abs (Figure 3D), but produced significantly increased levels of polyclonal IgG after immunization (Figure 3E).

TAPP KI B cells were previously found to have a relatively normal response to BCR cross-linking in vitro, with the exception of increased phosphorylation of the PI3K-dependant protein kinase Akt [35]. We thus further examined the GC B cell population to assess Akt phosphorylation, cell division and cell survival. Akt phosphorylation was examined by flow cytometry and found to be

significantly elevated within the TAPP KI GCB population (Figure 4A). GC B cell division was examined by pulse BrdU labeling and was not significantly altered (Figure 4B). TAPP KI GC B cells did however exhibit significantly increased cell viability ex vivo, based on DAPI and Annexin V staining (Figure 4C). Together these results suggested that uncoupling TAPP adaptors from the SHIP product PI(3,4)P2 results in abnormal levels of Akt phosphorylation and B cell survival within GC, which is is associated with larger GC size and increased production of non-Ag specific Abs.

**Ablation of GCs blocks development of autoantibodies in TAPP KI mice**

To investigate the role of chronic GCs in the development of autoantibody-mediated disease in TAPP KI mice, $ICOS^{-/-}$ mice [38] were crossed with TAPP KI mice to generate ICOS-/- TAPP KI mice or $ICOS^{+/-}$ TAPP KI mice. Immunization of young adult mice revealed that loss of one ICOS allele diminished the GC response in TAPP KI mice to levels comparable to wild-type control mice, while deletion of ICOS substantially ablated TAPP KI GC responses (Figure 5A). Development of chronic germinal centers in unimmunized middle-age TAPP KI mice showed a similar pattern of dependence on ICOS (Figure 5B). ICOS was also required for abnormal accumulation of the $CD80^{+}$ and $CD86^{+}$ B cell population (Figure 5C/D). Significantly, $ICOS^{-/-}$ TAPP KI mice did not show development of anti-dsDNA autoantibodies in the serum with age (Figure 5E/F). Anti-nuclear antibodies (Figure 5G) and IgG deposition in kidney (Figure 5H) were observed in TAPP KI mice but not in $ICOS^{-/-}$ TAPP KI mice. These results demonstrate that genetic disruption of chronic GC responses in TAPP KI mice impairs development of autoimmunity.

**B cell-intrinsic role of TAPP-PI(3,4)P2 interaction in preventing autoantibody production**

TAPP KI B cells were previously shown to be hyper-responsive to BCR cross-linking [35], suggesting that B cell-intrinsic signaling defects may underlie abnormal GC responses and development of autoantibodies in TAPP KI mice. We utilized an established mixed bone marrow chimera method [39] to reconstitute B cell deficient mice with either wild-type or TAPP KI B cells and thus assess whether TAPP KI B cells can drive autoimmune disease in an otherwise normal environment. Wild-type or TAPP KI bone marrow reconstituted the B cell compartment in μmT mice to a similar extent (Figure 6A), however circulating TAPP KI B cells showed increased levels of CD80 or CD86 within 6 weeks of reconstitution (Figure 6B). Unimmunized TAPP KI B cell chimeras developed increased GCB and Tfh populations in the spleen, as well as increased markers of chronic B cell activation compared to WT B cell chimeras (Figure 6C). TAPP KI B cell chimeric mice also exhibited circulating anti-dsDNA antibodies (Figure 6D), anti-nuclear antibodies (Figure 6E) and deposition of IgG in kidney glomeruli (Figure 6F). Together these results indicate that uncoupling TAPP adaptors from PI(3,4)P2 in B cells confers intrinsic hyper-activation properties that can drive autoimmune disease.

## Discussion

Autoimmune diseases such as SLE are characterized by chronic GC that are important for generation of mutated and class-switched autoantibodies [36, 40]. In TAPP KI mice we have detected a progressive increase in GCB cell frequencies with age as well as chronic activation of B cells based on increased expression of costimulatory molecules. Abnormal germinal centre responses can be driven by defects in either GCB or $T_{FH}$ subsets, which can bi-directionally activate each other and contribute to autoimmunity [41, 42]. Ablation of the GC response in TAPP KI mice by crossing with ICOS KO mice led to loss of anti-DNA Abs and also normalized the frequencies of CD80 or $CD86^{+}$ cells. This indicates that GCB-$T_{FH}$ interaction is critical for driving autoimmunity in this model, but does not resolve whether TAPP mutations in the B or T cell compartment is driving the response. Our μmT bone marrow chimera results indicate that uncoupling of TAPPs from PI(3,4)P2 in B cells is sufficient to drive chronic GCs (including expansion of the $T_{FH}$ population) and recapitulate the autoimmune phenotype of the TAPP KI mice. It remains possible that disruption of TAPP function in $T_{FH}$ cells or other immune cell populations may contribute to generation of the autoimmune or inflammatory state; this is a potential avenue of further investigation.

GC responses are highly dependent on PI3K signaling as demonstrated by PI3Kδ mutant mice that lack germinal centers [18, 19]. While proximal BCR signaling seems to be inhibited within most GC B cells, phosphorylation of Akt and its target S6K remains active in GC B cells [20], indicating that the PI3K/Akt pathway may have a critical role in GC B cells. Recent evidence indicates that PI3K and Akt are most active in the GC light zone and play a role in regulating isotype switch and selection of antigen-specific cells [43]. We previously found that TAPP KI B cells show elevated phosphorylation of Akt upon activation [35], thus our working hypothesis is that the abnormal GC

response in TAPP KI mice is a result of uncontrolled activity of Akt. Consistent with this hypothesis, we found increased Akt phosphorylation within TAPP KI GC B cells using phosflow analysis. Although TAPP KI mice form abnormally large GC upon immunization, their GCB cells did not show an increased in rate of DNA synthesis as assessed by BrdU labelling. In contrast, survival of GCB cells is significantly increased in TAPP KI mice, suggesting that dysregulation of Akt in TAPP KI cells may manifest as increased cell survival, whereas cell division may be controlled by other signaling molecules.

SHIP was found to be hyper-phosphorylated within GC B cells [20], likely via co-engagement of the BCR with FcγRIIB by immune complexes within the GC environment. This high activity of SHIP within GCB cells may result in rapid conversion of the PIP3 generated by PI3K into PI(3,4)P2, leaving primarily the latter phosphoinositide available to drive Akt activation. Binding of TAPP adaptors to PI(3,4)P2 may dampen Akt activation either by direct competition for this phosphoinositide, or by TAPP-mediated recruitment of other inhibitory molecules. TAPPs were reported to directly bind to the phosphatase PTPN13 (also known as PTPL1, FAP1 and PTP-BL), thus its possible that TAPPs regulate Akt via recruitment this phosphatase to the membrane [44]. TAPPs may additionally impact activity of PDK1, the upstream activating kinase for Akt, as PDK1 also binds to and is activated by PI(3,4)P2 [45].

A spectrum of chronic autoimmune diseases that includes SLE is associated with defective regulation of B cell activation and production of autoantibodies against DNA and nuclear proteins. Anti-DNA Abs frequently contain multiple somatic mutations, indicating their germinal center origin [40, 46]. Targeting B cells is an important strategy to improve treatment of SLE, however antibody-mediated B cell depletion or blockade of BAFF remain only marginally effective. Inhibition of B cell signaling pathways represents a new frontier beginning to be explored in

autoimmune disease [47]. Consistent with findings in other mouse models, our results indicate that deregulation of the PI3K/Akt pathway can lead to aberrant GCs and SLE-like disease. These findings suggest that targeting of PI3Ks and/or Akt may represent viable therapeutic strategies for treatment of SLE.

## Materials and methods

### Mice and immunizations

All animals were housed in a specific pathogen free facility at University of Manitoba, according to the Canadian Council on Animal Care guidelines. TAPP2$^{R211L/R211L}$ x TAPP2$^{R218L/R218L}$ (TAPP KI) mice contain mutations in the C-terminal PH domains of both TAPP1 and TAPP2 that abrogate their binding to the phosphoinositide PI(3,4)P2 as described [34]. p110δ$^{D910A/D910A}$ (p110d) mice contain a kinase-inactivating mutation in PI 3-kinase delta as described [19]. TAPP KI mice were crossed with mice deficient ICOS$^{-/-}$ mice to generate ICOS$^{-/-}$ x TAPP2$^{R211L/R211L}$ x TAPP2$^{R218L/R218L}$ triple mutant (ICOS$^{-/-}$ x TAPP KI) mice. B cell deficient μMT mice and ICOS$^{-/-}$ mice were purchased from Jackson Laboratory. Mice were used for the experiments between 6-12 weeks of age except where otherwise specified. To assess the acute development of GC, mice were injected intraperitoneally (i.p) with 2x10$^9$ sheep red blood cells (Cedarlane # CL2581-100A) or 10 ug of NP-OVA (Biosearch Technologies) precipitated in 2 mg of alum (Imject, Pierce Biotechnology).

### Flow cytometry

Spleens and mesenteric lymph nodes were homogenized to obtain single cell suspensions. RBCs were removed by using ACK lysis buffer. Cells were the filtered, re-suspended and counted to distribute 2 x 10$^6$ cells per FACS tube. Fc receptors were blocked by incubation with 2.4G2 monoclonal antibody for 30 min on ice prior to surface staining with the indicated antibodies. Anti-B220(PercpCy5.5), anti-CD19(V450), anti-CD4(V500), anti-GL7(FITC), anti-FAS (PE-Cy7), anti-CD80-APC, anti-CD86(APC), anti-Akt phospho-Ser308(PE), anti-PD1(biotin) and

anti-ICOS(APC) were purchased from BD Biosciences or eBiosciences and diluted in FACS buffer (PBS containing 2% FCS). For intracellular staining of phosphor-Akt, splenocytes were surface stained, treated with fix/perm buffer (BD Biosciences) and then stained with anti-Akt phospho-Ser308. Flow cytometry was performed using a BD FACS Canto II instrument. Data analyses were performed using FlowJo software.

**Assessment of germinal center responses**

For immunofluorescence microscopy analysis, spleens were harvested 14 days after NP-OVA immunization, embedded in O.C.T. compound (Tissue Tek) and snap frozen in liquid nitrogen. Frozen sections were fixed in ice cold acetone, blocked with 5% goat serum (30 min RT) and staining with biotinylated anti-IgD (2 hr RT), followed by streptavidin-Alexa 647, anti-GL7-FITC, and anti-CD4-PE (1hr RT). All staining reagents were diluted in PBS+2% BSA. Sections were imaged with an Ultraview LCI confocal microscope (Perkin-Elmer). The size of germinal centers were determined using image analysis software to calculate the relative areas of $GL7^+$ $IgD^-$ regions.

To measure in vivo DNA synthesis of germinal center B cells, mice were injected with 5 mg of 5-bromo-2'-deoxyuridine (BrdU) (Sigma Aldrich) in PBS 5 hours before sacrifice. After cell surface staining of splenocytes as described above, cells were fixed and permeabilized on ice for 30 min using BD Cytofix/Cytoperm solution, followed by PBS+1% saponin for 10 minutes. Sample were then treated with deoxyribonuclease I solution (0.15M NaCl, 4.2 mM $MgCl_2$, 10uM HCl, 50 Kunitz units/ml DNase I) for 30 minutes at 37°C and stained with FITC labeled anti-BrdU antibody (eBioscience). Ex vivo apoptosis was determined by staining with Annexin V-FITC (Biovision) and DAPI (Invitrogen). Surface stained splenocytes were resuspended in Annexin V Binding

Buffer (BD Pharmingen), and incubated with 1ul of Annexin V-FITC and 1ul DAPI (100ng/ul working solution) at RT for 10 minutes. Cells were then acquired immediately.

**ELISA**

Blood was collected by tail vein puncture or cardiac puncture and serum obtained after clotting centrifugation. For detection of total IgG and IgM, 96 well ELISA plates were coated with capture antibodies (Jackson ImmunoResearch) diluted in carbonate buffer (0.015M $Na_2CO_3$, 0.035 M $NaHCO_3$, 0.05% $NaN_3$, pH 9.6) overnight at $4^0$C. After blocking with 2% BSA in washing buffer (PBS, 0.05% Tween 20, 0.02% $NaN_3$, pH 7.4), incubation with diluted serum samples, and washing, bound antibodies were detected with biotinylated anti-mouse IgM or IgG antibodies (Southern Biotech). Antigen-specific antibodies binding to nitrophenyl (NP) were assayed by coating wells with $NP_3$-BSA or $NP_{20}$-BSA (Biosearch Technologies, Inc.) and detection with biotinylated antibodies specific for IgG1 (Southern Biotech). Plates were developed by incubation with streptavidin alkaline phosphatase, washing, addition of p-nitrophenyl phosphate substrate (Sigma Aldrich). Molecular Devices plate reader was used to measure the absorbance at 405nm and 690nm. Anti-dsDNA IgG antibodies were measured using a kit from Alpha Diagnostics International, according to the manufacturers protocol.

**Anti-nuclear antibodies and IgG deposition in kidney**

Serum was obtained from peripheral blood of middle-aged mice after cardiac puncture. Antinuclear antibodies within the serum were detected by staining slides coated with HEp-2 cells (Biorad, cat# 26102). Slides were blocked for one hour with normal horse serum, then serum samples diluted 1:40 were added and slides incubated for 2 hrs. After washing with PBST (0.01%

Tween in PBS), FITC tagged rabbit anti-mouse IgG secondary antibody (Life Technologies) was added at 1:2000 dilution. Slides were incubated for 30 mins, washed and mounted using ProLong Gold anti-fade reagent (Molecular Probes). To detect deposition of IgG within the kidney, freshly harvested kidneys were embedded in OCT and snap frozen in liquid nitrogen. 8 uM thick cryosections were prepared and stored at -80 C. Sections were fixed in cold acetone prior to staining with rabbit polyclonal anti mouse IgG at 1:2000 dilutions. For all staining procedures, antibodies were diluted in PBS containing 0.1% BSA and 0.01% Tween20. Slides were imaged using a Zeiss AxioObserver spinning disk confocal microscope.

**Generation of bone marrow chimeras**

Bone marrow chimeras containing wild-type or TAPP KI B cells were generated as described [39]. Briefly, 6-8 week old uMT mice were lethally irradiated in a RS2000 irradiator (Rad Source Technologies), using two doses of 450 cGy separated by 2hr. Bone marrow (BM) harvested from 4-6 week old WT or TAPP1/2 KI mice and the BM cells were mixed with uMT BM at a 1:4 ratio and used to reconstitute irradiated umT mice.

**Statistical analysis**

Statistical analysis was performed with GraphPad Prism software. P values were calculated using two-tailed unpaired student's T test unless specified. Figures use the following representation for significance *P< 0.05, **P< 0.001, ***P< 0.0001

## Acknowledgements

We thank Stephen Wullschleger for generation of TAPP KI mice and Drs. John Cambier and Tingting Zhang for critical reading of the manuscript. A.J.M. is the Canada Research Chair in Molecular Immunology. This work was supported by the Canadian Institutes of Health Research (MOP-93771).

## Conflict of Interest Disclosure

The authors declare no commercial or financial conflict of interest.

## Figure Legends

**Figure 1. TAPP1/2 KI mice develop chronic B cell activation and chronic GCs with age.**
A cohort of wild-type (WT) or TAPP2$^{R211L/R211L}$ x TAPP2$^{R218L/R218L}$ (TAPP KI) mice and p110δ$^{D910A/D910A}$ (p110d) mice were examined at 28-30 weeks of age. Splenocytes or mesenteric lymph node cells harvested from these mice and were analyzed by flow cytometry. (A) Splenic GL7$^{+}$Fas$^{+}$ germinal center B cells (GCB) were assessed as a percent of B220$^{+}$ B cells (for gating details see Supplementary Fig. 1). Representative dot plots are shown at left and summary graph is shown on the right. (B) Splenic PD1$^{+}$ ICOS$^{+}$ $T_{FH}$ subsets were assessed as a percent of CD4$^{+}$ T cells. Representative dot plots are shown at left and summary graph is shown on the right. (C) Expression of activation/memory markers CD80 and CD86 within splenic B220+ cells (representative histograms and gating shown in Supplementary Figure 2). (D) Frequencies of GCB cells, CD80 and CD86 expressing B cells within mesenteric lymph node were determined using the same method as for splenocytes. Data are pooled from two independent experiments totaling 6-7 mice per group. TAPP KI versus WT statistical comparisons were performed by two tailed T-test and significance is indicated as NS P>0.05, *P< 0.05, **P< 0.001, ***P< 0.0001.

**Figure 2. Development of chronic GC in TAPP KI mice is age and gene dose dependent**
Spleens were harvested from unimmunized young adult (8-12 wk), middle aged (28-30 wk) and old (42-45 wk) mice, and analyzed by flow cytometry. (A) Percentage of GCB cells in WT, TAPP KI and p110δ KI mice in the indicated age groups. (B) Percentage of TFH population in the indicated age groups of WT, TAPP KI and p110δ KI mice. (C) Effect of mutant TAPP1 and TAPP2 gene dose on GCB cell frequencies in young adult mice. (D) Effect of mutant TAPP gene dose on TFH frequencies in young adult mice. (E) Age-dependent expression of CD80 in B cells.

(F) Effect of mutant TAPP gene dose on CD80 expression in B cells from naïve young adults. Graphs A, B and E represent the mean and standard error of 3-7 mice per time point pooled from 2 independent experiments, and statistical comparisons between TAPP KI versus WT were performed by two-way ANOVA. Graphs C, D and F represent the mean and standard error of 3-7 mice per genotype pooled from 3 independent experiments, and statistical comparisons between homozygous TAPP KI and the indicated heterozygous genotypes or were performed by two-tailed T-test. Significance is indicated as NS P>0.05, *P< 0.05, **P< 0.001, ***P< 0.0001.

**Figure 3. Increased GC size generated upon immunization of young adult TAPP KI mice.**

Young adult WT or TAPP KI mice (8-12 weeks of age) were immunized with sheep red blood cells (SRBC) or with nitrophenyl-ovalbumin precipitated in alum (NP-OVA/alum) and analyzed 8 or 10 days later respectively. (A) Spleens were harvested and the frequency of $GL7^{+}FAS^{+}$ germinal center B cells (GCB) determined by flow cytometry. Bar graph shows GCB frequencies as a percent of total B cells, with GCB-deficient $p110\delta^{D910A/D910A}$ (p110d) mice used as controls. Results are from a single experiment with 4 mice per group and are representative of 3 similar experiments. (B) Spleen cryosections from NP-OVA/alum-immunized mice were stained to detect $GL7^{+}IgD^{-}$ GCs by confocal microscopy. Graph shows the relative area of GCs pooled from 3 mice per genotype. Each dot represents pixel count for a region of interest encompassing one GC. Scale bars, 200 μm. (C) The $PD1^{+}ICOS^{+}$ $T_{FH}$ population was assessed in SRBC immunized mice. Graph displays the percentage of $T_{FH}$ cells among $CD4^{+}$ T cells from individual mice of the indicated genotypes. Data are pooled from 2 experiments, each with 3 WT and TAPP KI mice. (D) Sera were collected from NP-OVA/alum immunized mice at day 14, 21, 28 and 35 and analyzed by ELISA for binding to NP3-BSA or NP20-BSA to detect high and low affinity antigen-specific antibody respectively. Graph shows the ratio of NP3/NP20 binding IgG Ab over time after

immunization. (E) Total IgG antibody levels from the same immunized mice as in D. TAPP KI versus WT statistical comparisons were performed by two tailed T-test (A-C) or two-way ANOVA (E) and significance is indicated as *P< 0.05, **P< 0.001, ***P< 0.0001.

**Figure 4. TAPP KI GC B cells show normal proliferation but increased Akt phosphorylation and survival**

(A) Splenocytes were surface stained, fixed, permeabilized and intracellularly stained with anti-phosphoAkt. Histograms of anti-phosphoAkt staining within the GCB population are shown for two representative TAPP KI or WT mice from the same experiment. The right panel shows average anti-phosphoAkt mean fluorescence intensity (MFI) within GCB or non-GCB populations, pooled from 2 experiments with 3 mice per experiment. (B) OVA/alum-immunized mice were injected with BrdU five hours before sacrifice on day 14. Cells were then surface-stained, fixed, permeabilized and then intracellularly stained with anti-BrdU to determine BrdU incorporation within the GCB and non-GCB populations by flow cytometry. (C) To assess cell survival ex vivo, the frequency of annexin V and DAPI negative cells among GCB and non-GCB populations was determined by flow cytometry. The AnnexinV/DAPI density plots are representative of 2 experiments each with 3 mice per group. The graph on the right shows the frequencies of annexinV and DAPI negative cells among GCB from individual WT and TAPP KI mice at the indicated time points after immunization. All data show representative experiments containing at least 3 mice per group. TAPP KI versus WT statistical comparisons were performed using 2-tailed T-test and significance is indicated as NS P>0.05, *P< 0.05, **P< 0.001, ***P< 0.0001.

**Figure 5. Ablation of GCs blocks development of autoantibodies in TAPP KI mice.**

(A) Young adult mice TAPP KI or ICOS $^{-/-}$ x TAPP KI mice were immunized with sheep red blood cells and analyzed for B220$^{+}$GL7$^{+}$FAS$^{+}$ GCB cells at day 8 by flow cytometry. Results are pooled from 2 experiments, each with 3 mice per genotype. (B) Middle aged TAPP KI or ICOS $^{-/-}$ TAPP KI mice were analyzed for chronic GCB. (C, D) Expression of CD80 and CD86. Results in B-D are pooled from 3 experiments, totaling 3-5 mice per genotype. TAPP KI versus ICOS $^{-/-}$ x TAPP KI statistical comparisons were performed using two tailed T-test and significance is indicated as **P< 0.001, ***P< 0.0001. (E, F) Sera collected from mice at the indicated age were tested by ELISA for (E) anti-double stranded DNA IgG or (F) anti-double stranded DNA IgM. Results are pooled from 3-4 mice per genotype each undergoing multiple serum collections at the indicated time points. TAPP KI versus ICOS $^{-/-}$ x TAPP KI statistical comparisons were performed using 2-way ANOVA and significance is indicated as *P< 0.05, ***P< 0.0001. (G) Sera obtained from middle aged mice were tested for anti-nuclear antibodies by immunofluorescence staining of HEp2 cells. Images are representative of 3 mice tested per genotype. (H) Kidney cryosections from middle aged mice were stained for IgG antibody to detect immune complex deposition in glomeruli. Images are representative of 3 mice tested per genotype. Scale bars, 20 μm.

**Figure 6. TAPP KI B cells can drive the development of autoimmunity**

Irradiated B cell-deficient (μmT) mice were reconstituted with a mixture of either TAPP KI or WT bone marrow and μmT bone marrow at a 1:4 ratio. Blood cells were collected from recipient μmT mice at 6 weeks post-reconstitution and then analyzed by flow cytometry to determine (A) reconstitution of B cells and (B) B-cell expression of CD80 and CD86 (right). (C) At 25 weeks post-reconstitution, splenic B cells from these mice were analyzed for GCB, CD80$^{+}$ and CD86$^{+}$ B-cell populations (left) and $T_{fh}$ cells (right). (D) Sera from B cell reconstituted mice were collected at 15, 20 and 25 weeks and tested by ELISA for anti-dsDNA IgG antibody. (E) At 25

weeks post-reconstitution, sera were tested for anti-nuclear antibody by immunofluorescence staining of HEp2 cells. (F) At 25 weeks post-reconstitution, kidney sections were tested for IgG immune complex deposition. Images in E and F are representative of 3 mice tested per group. Graphs A-D are results pooled from 2 experiments, each with 3 mice. TAPP KI versus WT statistical comparisons were performed by two tailed T-test (A-C) or two-way ANOVA (D) and significance is indicated as NS $P>0.05$, *$P< 0.05$, **$P< 0.001$, ***$P< 0.0001$.

# References


1 **So, L. and Fruman, D. A.,** PI3K signalling in B- and T-lymphocytes: new developments and therapeutic advances. *The Biochemical journal*. 2012. **442**: 465-481.

2 **Koyasu, S.,** Role of class IA phosphoinositide 3-kinase in B lymphocyte development and functions. *Biochemical Society transactions*. 2004. **32**: 320-325.

3 **Werner, M., Hobeika, E. and Jumaa, H.,** Role of PI3K in the generation and survival of B cells. *Immunological reviews*. 2010. **237**: 55-71.

4 **Pauls, S. D., Lafarge, S. T., Landego, I., Zhang, T. and Marshall, A. J.,** The phosphoinositide 3-kinase signaling pathway in normal and malignant B cells: activation mechanisms, regulation and impact on cellular functions. *Front Immunol*. 2012. **3**: 224.

5 **Dyson, J. M., Fedele, C. G., Davies, E. M., Becanovic, J. and Mitchell, C. A.,** Phosphoinositide phosphatases: just as important as the kinases. *Subcell Biochem*. 2012. **58**: 215-279.

6 **Lam, K. P., Kuhn, R. and Rajewsky, K.,** In vivo ablation of surface immunoglobulin on mature B cells by inducible gene targeting results in rapid cell death. *Cell*. 1997. **90**: 1073-1083.

7 **Srinivasan, L., Sasaki, Y., Calado, D. P., Zhang, B., Paik, J. H., DePinho, R. A., Kutok, J. L. *et al.*,** PI3 kinase signals BCR-dependent mature B cell survival. *Cell*. 2009. **139**: 573-586.

8 **Puri, K. D. and Gold, M. R.,** Selective inhibitors of phosphoinositide 3-kinase delta: modulators of B-cell function with potential for treating autoimmune inflammatory diseases and B-cell malignancies. *Frontiers in immunology*. 2012. **3**: 256.

9 **Helgason, C. D., Kalberer, C. P., Damen, J. E., Chappel, S. M., Pineault, N., Krystal, G. and Humphries, R. K.,** A dual role for Src homology 2 domain-containing inositol-5-phosphatase (SHIP) in immunity: aberrant development and enhanced function of b lymphocytes in ship -/- mice. *The Journal of experimental medicine*. 2000. **191**: 781-794.

10 **Brauweiler, A., Tamir, I., Dal Porto, J., Benschop, R. J., Helgason, C. D., Humphries, R. K., Freed, J. H. *et al.*,** Differential regulation of B cell development, activation, and death by the src homology 2 domain-containing 5' inositol phosphatase (SHIP). *The Journal of experimental medicine*. 2000. **191**: 1545-1554.

11 **O'Neill, S. K., Getahun, A., Gauld, S. B., Merrell, K. T., Tamir, I., Smith, M. J., Dal Porto, J. M. *et al.*,** Monophosphorylation of CD79a and CD79b ITAM motifs initiates a SHIP-1 phosphatase-mediated inhibitory signaling cascade required for B cell anergy. *Immunity*. 2011. **35**: 746-756.

12 **Akerlund, J., Getahun, A. and Cambier, J. C.,** B cell expression of the SH2-containing inositol 5-phosphatase (SHIP-1) is required to establish anergy to high affinity, proteinacious autoantigens. *J Autoimmun*. 2015. **62**: 45-54.

13 **Ono, M., Okada, H., Bolland, S., Yanagi, S., Kurosaki, T. and Ravetch, J. V.,** Deletion of SHIP or SHP-1 reveals two distinct pathways for inhibitory signaling. *Cell*. 1997. **90**: 293-301.

14 **Li, R., Peng, H., Chen, G. M., Feng, C. C., Zhang, Y. J., Wen, P. F., Qiu, L. J. *et al.*,** Association of FCGR2A-R/H131 polymorphism with susceptibility to systemic lupus erythematosus among Asian population: a meta-analysis of 20 studies. *Archives of dermatological research*. 2014. **306**: 781-791.

15 **Boross, P., Arandhara, V. L., Martin-Ramirez, J., Santiago-Raber, M. L., Carlucci, F., Flierman, R., van der Kaa, J. *et al.*,** The inhibiting Fc receptor for IgG, FcgammaRIIB, is a modifier of autoimmune susceptibility. *Journal of immunology*. 2011. **187**: 1304-1313.

16 **Rahman, Z. S., Niu, H., Perry, D., Wakeland, E., Manser, T. and Morel, L.,** Expression of the autoimmune Fcgr2b NZW allele fails to be upregulated in germinal center B cells and is associated with increased IgG production. *Genes and immunity*. 2007. **8**: 604-612.

17 **Rolf, J., Bell, S. E., Kovesdi, D., Janas, M. L., Soond, D. R., Webb, L. M., Santinelli, S. *et al.*,** Phosphoinositide 3-kinase activity in T cells regulates the magnitude of the germinal center reaction. *J Immunol*. 2010. **185**: 4042-4052.

18 **Jou, S. T., Carpino, N., Takahashi, Y., Piekorz, R., Chao, J. R., Wang, D. and Ihle, J. N.,** Essential, nonredundant role for the phosphoinositide 3-kinase p110delta in signaling by the B-cell receptor complex. *Molecular and cellular biology*. 2002. **22**: 8580-8591.

19 **Okkenhaug, K., Bilancio, A., Farjot, G., Priddle, H., Sancho, S., Peskett, E., Pearce, W. *et al.*,** Impaired B and T cell antigen receptor signaling in p110delta PI 3-kinase mutant mice. *Science*. 2002. **297**: 1031-1034.

20 **Khalil, A. M., Cambier, J. C. and Shlomchik, M. J.,** B cell receptor signal transduction in the GC is short-circuited by high phosphatase activity. *Science*. 2012. **336**: 1178-1181.

21 **Vikstrom, I., Carotta, S., Luthje, K., Peperzak, V., Jost, P. J., Glaser, S., Busslinger, M. *et al.*,** Mcl-1 is essential for germinal center formation and B cell memory. *Science*. 2010. **330**: 1095-1099.

22 **Zhang, T. T., Makondo, K. J. and Marshall, A. J.,** p110delta phosphoinositide 3-kinase represses IgE switch by potentiating BCL6 expression. *J Immunol*. 2012. **188**: 3700-3708.

23 **Omori, S. A., Cato, M. H., Anzelon-Mills, A., Puri, K. D., Shapiro-Shelef, M., Calame, K. and Rickert, R. C.,** Regulation of class-switch recombination and plasma cell differentiation by phosphatidylinositol 3-kinase signaling. *Immunity*. 2006. **25**: 545-557.

24 **Hammond, G. R. and Balla, T.,** Polyphosphoinositide binding domains: Key to inositol lipid biology. *Biochim Biophys Acta*. 2015. **1851**: 746-758.

25 **Zhang, T. T., Li, H., Cheung, S. M., Costantini, J. L., Hou, S., Al-Alwan, M. and Marshall, A. J.,** Phosphoinositide 3-kinase-regulated adapters in lymphocyte activation. *Immunol Rev*. 2009. **232**: 255-272.

26 **Frech, M., Andjelkovic, M., Ingley, E., Reddy, K. K., Falck, J. R. and Hemmings, B. A.,** High affinity binding of inositol phosphates and phosphoinositides to the pleckstrin homology domain of RAC/protein kinase B and their influence on kinase activity. *J Biol Chem*. 1997. **272**: 8474-8481.

27 **Rameh, L. E., Arvidsson, A., Carraway, K. L., 3rd, Couvillon, A. D., Rathbun, G., Crompton, A., VanRenterghem, B. *et al.*,** A comparative analysis of the phosphoinositide binding specificity of pleckstrin homology domains. *J Biol Chem*. 1997. **272**: 22059-22066.

28 **Franke, T. F., Kaplan, D. R., Cantley, L. C. and Toker, A.,** Direct regulation of the Akt proto-oncogene product by phosphatidylinositol-3,4-bisphosphate. *Science*. 1997. **275**: 665-668.

29 **Thomas, C. C., Dowler, S., Deak, M., Alessi, D. R. and van Aalten, D. M.,** Crystal structure of the phosphatidylinositol 3,4-bisphosphate-binding pleckstrin homology (PH) domain of tandem PH-domain-containing protein 1 (TAPP1): molecular basis of lipid specificity. *The Biochemical journal*. 2001. **358**: 287-294.

30 **Marshall, A. J., Krahn, A. K., Ma, K., Duronio, V. and Hou, S.,** TAPP1 and TAPP2 are targets of phosphatidylinositol 3-kinase signaling in B cells: sustained plasma membrane recruitment triggered by the B-cell antigen receptor. *Molecular and cellular biology*. 2002. **22**: 5479-5491.

31 **Bolland, S., Pearse, R. N., Kurosaki, T. and Ravetch, J. V.,** SHIP modulates immune receptor responses by regulating membrane association of Btk. *Immunity*. 1998. **8**: 509-516.

32 **Liu, Q., Oliveira-Dos-Santos, A. J., Mariathasan, S., Bouchard, D., Jones, J., Sarao, R., Kozieradzki, I. *et al.*,** The inositol polyphosphate 5-phosphatase ship is a crucial negative regulator of B cell antigen receptor signaling. *The Journal of experimental medicine*. 1998. **188**: 1333-1342.

33 **Krahn, A. K., Ma, K., Hou, S., Duronio, V. and Marshall, A. J.,** Two distinct waves of membrane-proximal B cell antigen receptor signaling differentially regulated by Src homology 2-containing inositol polyphosphate 5-phosphatase. *J Immunol*. 2004. **172**: 331-339.

34 **Wullschleger, S., Wasserman, D. H., Gray, A., Sakamoto, K. and Alessi, D. R.,** Role of TAPP1 and TAPP2 adaptor binding to PtdIns(3,4)P2 in regulating insulin sensitivity defined by knock-in analysis. *The Biochemical journal*. 2011. **434**: 265-274.

35 **Landego, I., Jayachandran, N., Wullschleger, S., Zhang, T. T., Gibson, I. W., Miller, A., Alessi, D. R. *et al.*,** Interaction of TAPP adapter proteins with phosphatidylinositol (3,4)-bisphosphate regulates B-cell activation and autoantibody production. *European journal of immunology*. 2012. **42**: 2760-2770.

36 **Luzina, I. G., Atamas, S. P., Storrer, C. E., daSilva, L. C., Kelsoe, G., Papadimitriou, J. C. and Handwerger, B. S.,** Spontaneous formation of germinal centers in autoimmune mice. *Journal of leukocyte biology*. 2001. **70**: 578-584.

37 **Grammer, A. C., Slota, R., Fischer, R., Gur, H., Girschick, H., Yarboro, C., Illei, G. G. *et al.*,** Abnormal germinal center reactions in systemic lupus erythematosus demonstrated by blockade of CD154-CD40 interactions. *The Journal of clinical investigation*. 2003. **112**: 1506-1520.

38 **Tafuri, A., Shahinian, A., Bladt, F., Yoshinaga, S. K., Jordana, M., Wakeham, A., Boucher, L. M. *et al.*,** ICOS is essential for effective T-helper-cell responses. *Nature*. 2001. **409**: 105-109.

39 **Becker-Herman, S., Meyer-Bahlburg, A., Schwartz, M. A., Jackson, S. W., Hudkins, K. L., Liu, C., Sather, B. D. *et al.*,** WASp-deficient B cells play a critical, cell-intrinsic role in triggering autoimmunity. *The Journal of experimental medicine*. 2011. **208**: 2033-2042.

40 **Guo, W., Smith, D., Aviszus, K., Detanico, T., Heiser, R. A. and Wysocki, L. J.,** Somatic hypermutation as a generator of antinuclear antibodies in a murine model of systemic autoimmunity. *The Journal of experimental medicine*. 2010. **207**: 2225-2237.

41 **Cannons, J. L., Qi, H., Lu, K. T., Dutta, M., Gomez-Rodriguez, J., Cheng, J., Wakeland, E. K. *et al.*,** Optimal germinal center responses require a multistage T cell:B cell adhesion process involving integrins, SLAM-associated protein, and CD84. *Immunity*. 2010. **32**: 253-265.

42 **Pratama, A. and Vinuesa, C. G.,** Control of TFH cell numbers: why and how? *Immunol Cell Biol*. 2014. **92**: 40-48.

43 **Sander, S., Chu, V. T., Yasuda, T., Franklin, A., Graf, R., Calado, D. P., Li, S. *et al.*,** PI3 Kinase and FOXO1 Transcription Factor Activity Differentially Control B Cells in the Germinal Center Light and Dark Zones. *Immunity*. 2015. **43**: 1075-1086.

44 **Kimber, W. A., Deak, M., Prescott, A. R. and Alessi, D. R.,** Interaction of the protein tyrosine phosphatase PTPL1 with the PtdIns(3,4)P2-binding adaptor protein TAPP1. *The Biochemical journal*. 2003. **376**: 525-535.

45 **Currie, R. A., Walker, K. S., Gray, A., Deak, M., Casamayor, A., Downes, C. P., Cohen, P. *et al.*,** Role of phosphatidylinositol 3,4,5-trisphosphate in regulating the activity and localization of 3-phosphoinositide-dependent protein kinase-1. *The Biochemical journal*. 1999. **337 ( Pt 3)**: 575-583.

46 **Wellmann, U., Letz, M., Herrmann, M., Angermuller, S., Kalden, J. R. and Winkler, T. H.,** The evolution of human anti-double-stranded DNA autoantibodies. *Proceedings of the National Academy of Sciences of the United States of America*. 2005. **102**: 9258-9263.

47 **Puri, K. D., Di Paolo, J. A. and Gold, M. R.,** B-cell receptor signaling inhibitors for treatment of autoimmune inflammatory diseases and B-cell malignancies. *Int Rev Immunol*. 2013. **32**: 397-427.

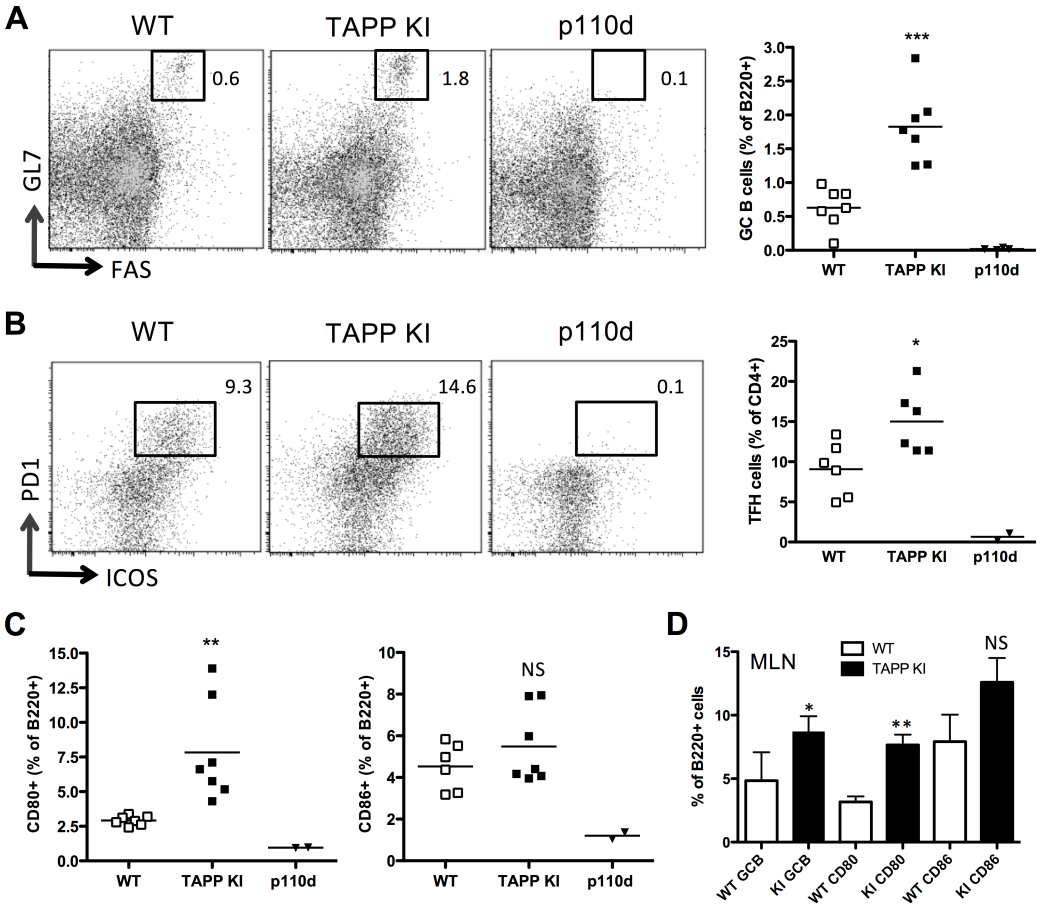
A
WT
TAPP KI
p110d
0.6
1.8
0.1
GL7
FAS
GC B cells (% of B220+)
***
WT
TAPP KI
p110d
B
WT
TAPP KI
p110d
9.3
14.6
0.1
PD1
ICOS
TFH cells (% of CD4+)
*
WT
TAPP KI
p110d
C
CD80+ (% of B220+)
**
WT
TAPP KI
p110d
CD86+ (% of B220+)
NS
WT
TAPP KI
p110d
D
MLN
WT
TAPP KI
% of B220+ cells
*
**
NS
WT GCB
KI GCB
WT CD80
KI CD80
WT CD86
KI CD86

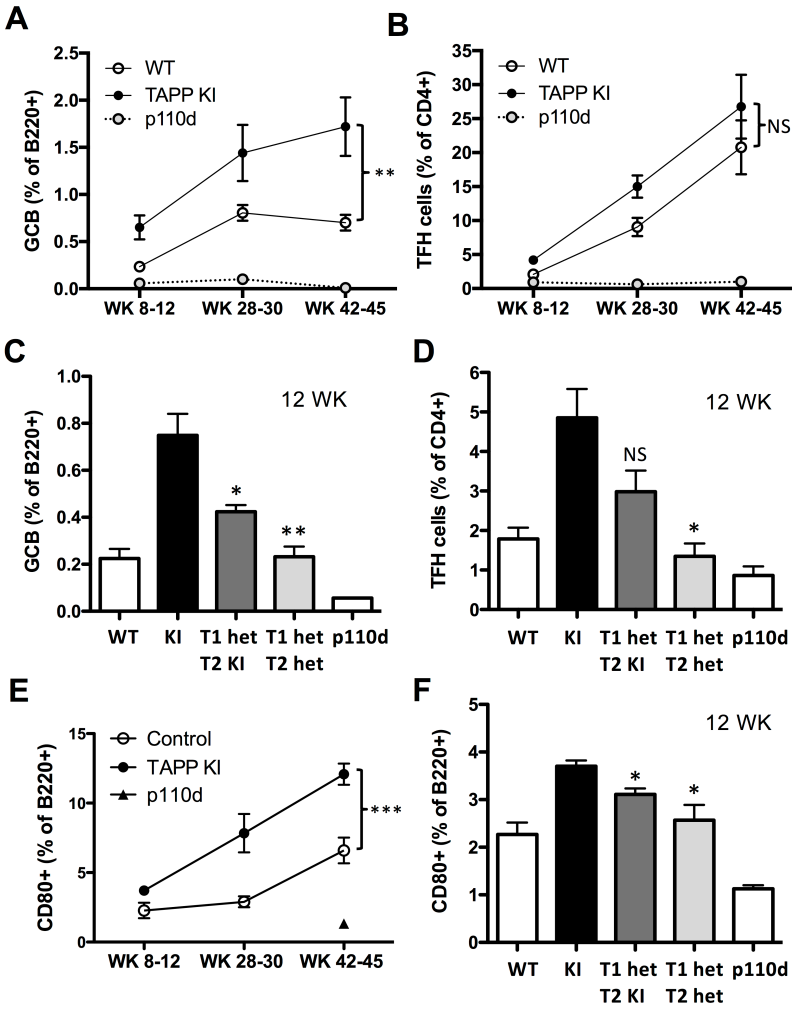
A
GCB (% of B220+)
WT
TAPP KI
p110d
**
WK 8-12
WK 28-30
WK 42-45
B
TFH cells (% of CD4+)
NS
C
12 WK
*
**
WT
KI
T1 het T2 KI
T1 het T2 het
p110d
D
NS
E
CD80+ (% of B220+)
Control
***
F

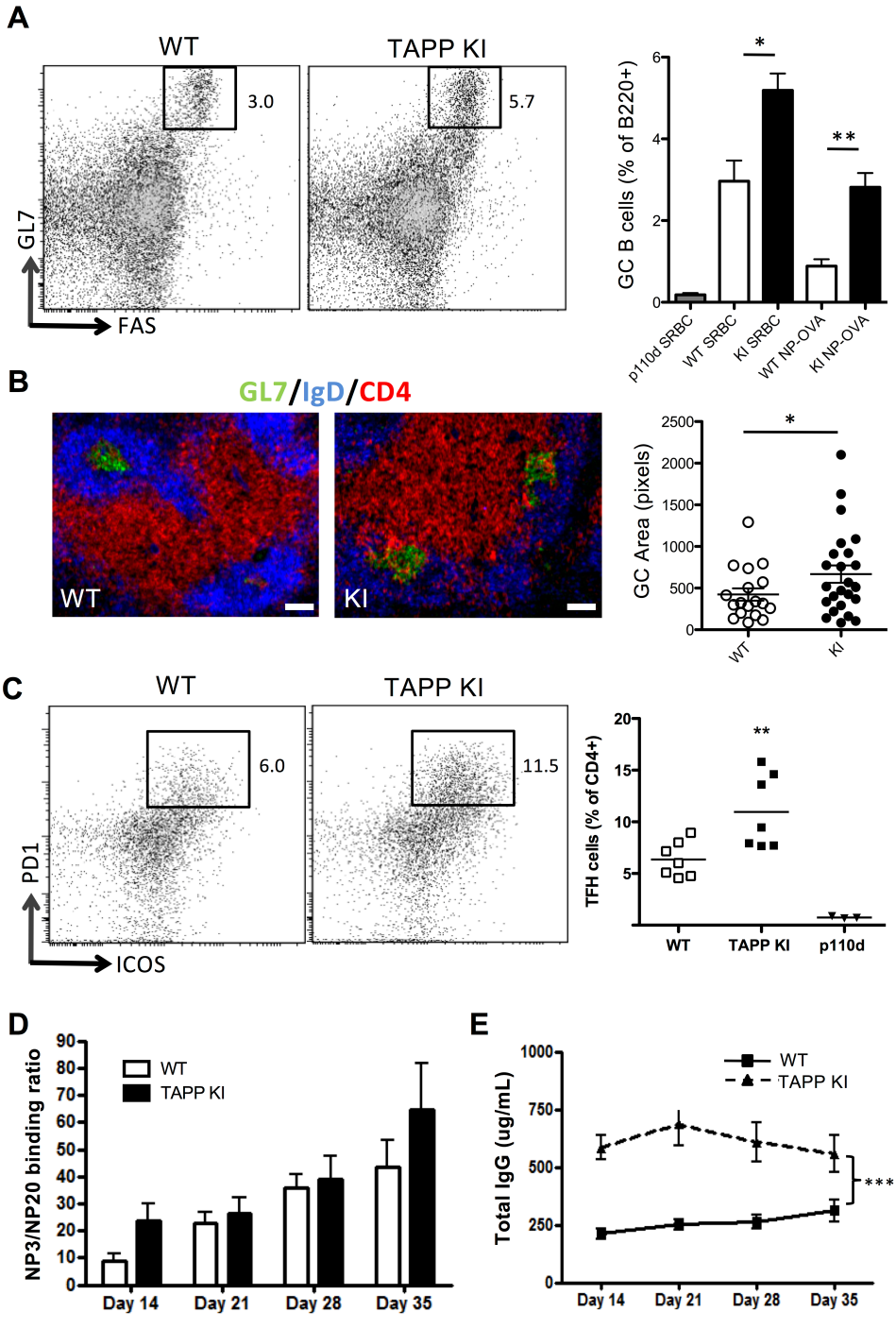
A
WT
TAPP KI
3.0
5.7
GL7
FAS
GC B cells (% of B220+)
p110d SRBC
WT SRBC
KI SRBC
WT NP-OVA
KI NP-OVA
B
GL7/IgD/CD4
WT
KI
GC Area (pixels)
C
WT
TAPP KI
6.0
11.5
PD1
ICOS
TFH cells (% of CD4+)
WT
TAPP KI
p110d
D
NP3/NP20 binding ratio
WT
TAPP KI
Day 14
Day 21
Day 28
Day 35
E
Total IgG (ug/mL)
WT
TAPP KI
Day 14
Day 21
Day 28
Day 35

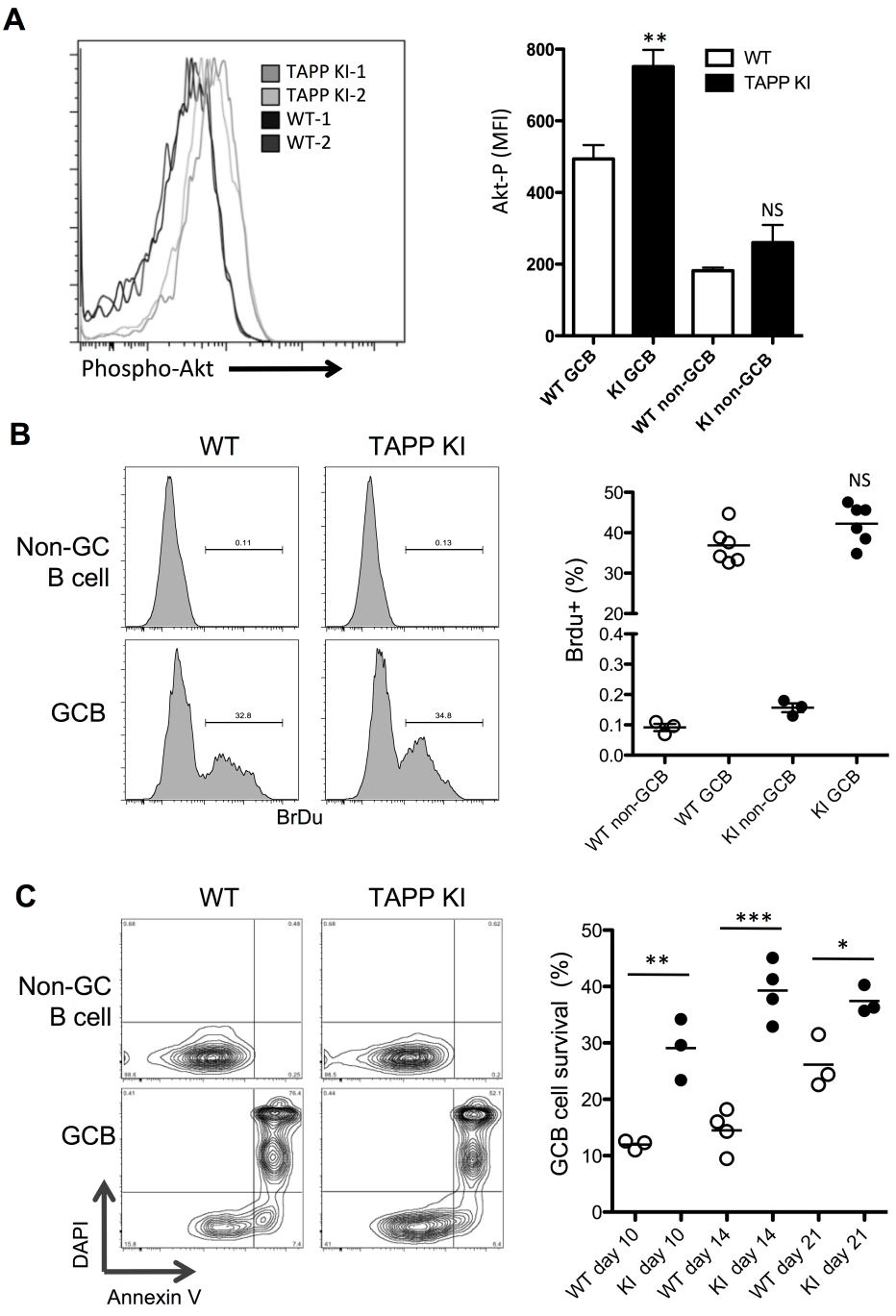
A
TAPP KI-1
TAPP KI-2
WT-1
WT-2
Phospho-Akt
Akt-P (MFI)
WT
TAPP KI
**
NS
WT GCB
KI GCB
WT non-GCB
KI non-GCB
B
WT
TAPP KI
Non-GC B cell
GCB
0.11
0.13
32.8
34.8
BrDu
Brdu+ (%)
NS
WT non-GCB
WT GCB
KI non-GCB
KI GCB
C
WT
TAPP KI
Non-GC B cell
GCB
DAPI
Annexin V
GCB cell survival (%)
**
***
*
WT day 10
KI day 10
WT day 14
KI day 14
WT day 21
KI day 21

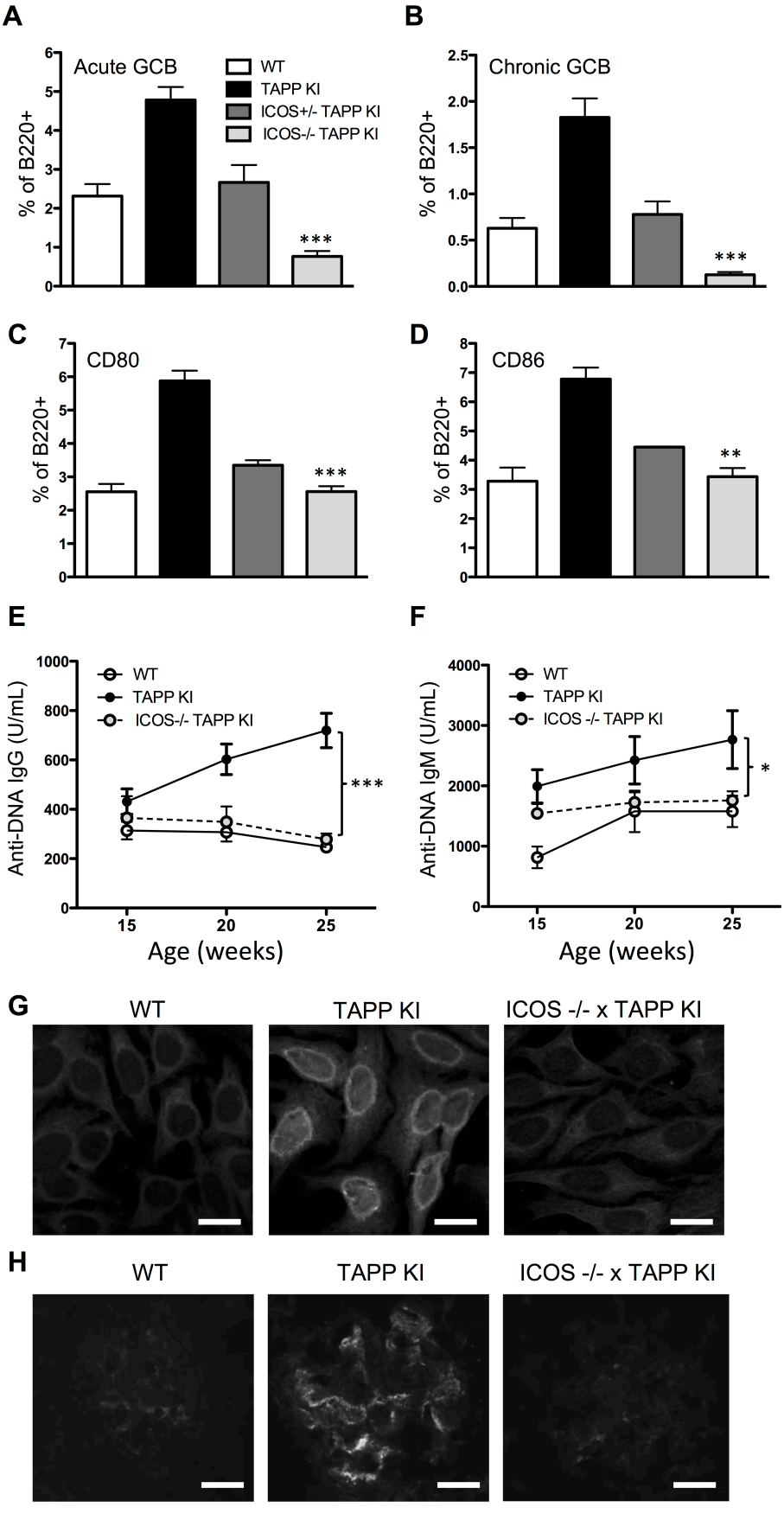
A
Acute GCB
WT
TAPP KI
ICOS+/- TAPP KI
ICOS-/- TAPP KI
% of B220+
***
B
Chronic GCB
% of B220+
***
C
CD80
% of B220+
***
D
CD86
% of B220+
**
E
Anti-DNA IgG (U/mL)
WT
TAPP KI
ICOS-/- TAPP KI
***
Age (weeks)
F
Anti-DNA IgM (U/mL)
WT
TAPP KI
ICOS -/- TAPP KI
*
Age (weeks)
G
WT
TAPP KI
ICOS -/- x TAPP KI
H
WT
TAPP KI
ICOS -/- x TAPP KI

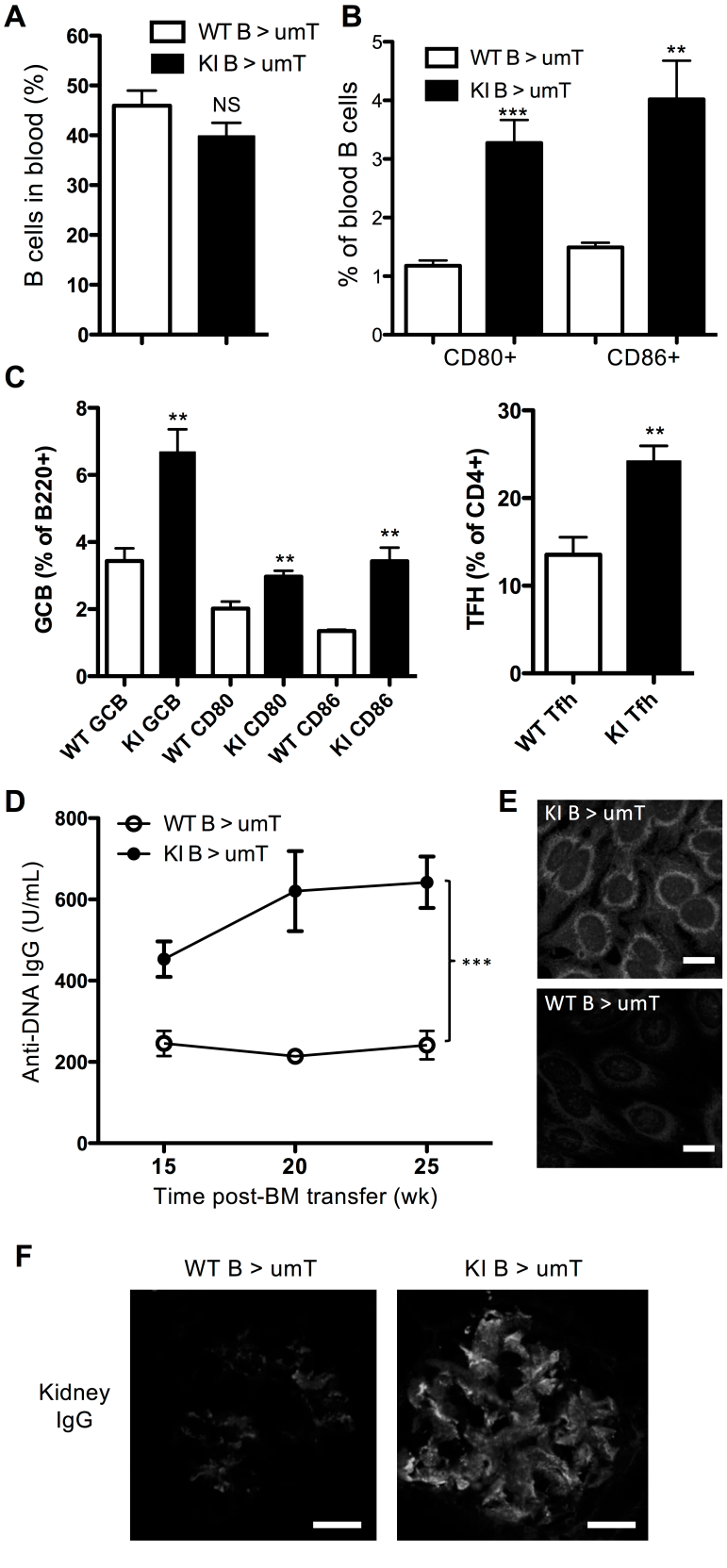
A
WT B > umT
KI B > umT
B cells in blood (%)
NS
B
% of blood B cells
***
**
CD80+
CD86+
C
GCB (% of B220+)
WT GCB
KI GCB
WT CD80
KI CD80
WT CD86
KI CD86
TFH (% of CD4+)
WT Tfh
KI Tfh
D
Anti-DNA IgG (U/mL)
Time post-BM transfer (wk)
E
KI B > umT
WT B > umT
F
WT B > umT
KI B > umT
Kidney IgG

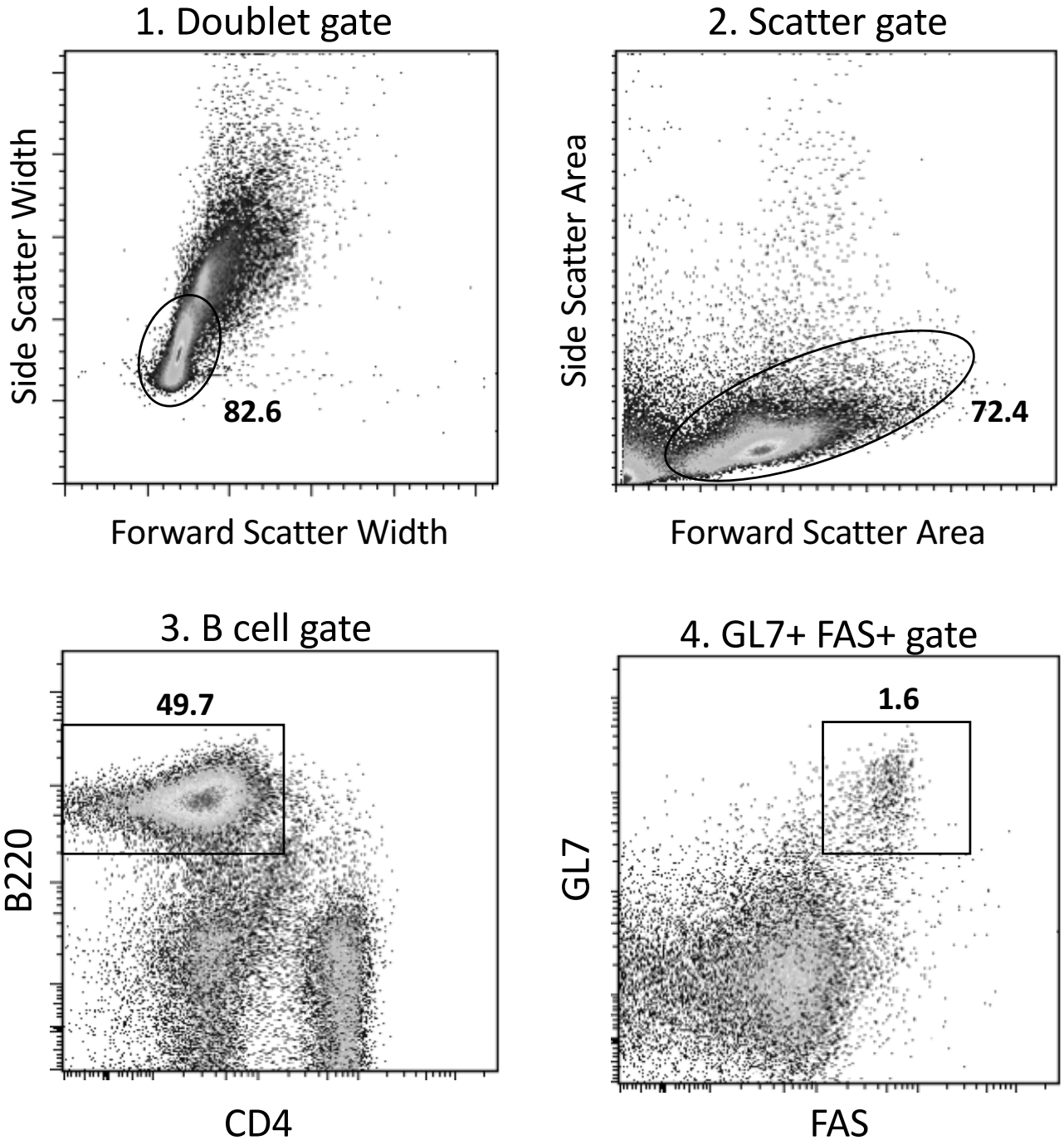


**Supplementary Figure 1. Strategy for gating germinal center B cells.**
An example of splenocytes stained for B220, CD4, GL7 and Fas is shown. Two steps of scatter gating were used as illustrated to remove doublets, high side scatter granulocytes and dead cells from the analysis. The third and fourth gates were used to identify total B220+CD4- B cells and GL7+Fas+ germinal center B cells. In all data figures, germinal center B cells (GCB) are expressed as the percent of the total B220+ B cells.

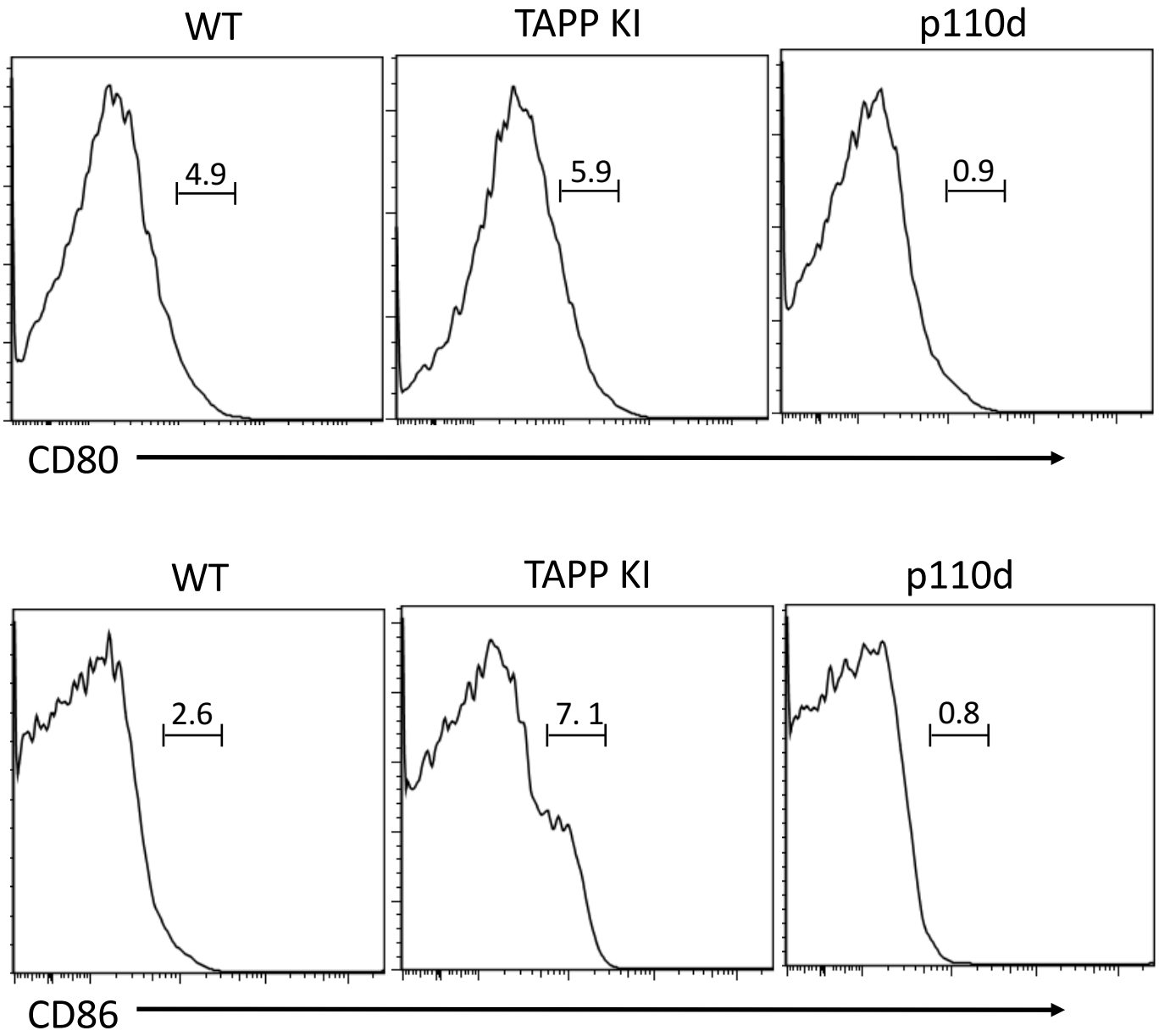


**Supplementary Figure 2. Increased CD80 and CD86 expression on B cells from TAPP KI mice.**

Histograms show expression of CD80 or CD86 on B220+ splenic B cells from representative wild-type C57BL6 (WT*)*, TAPP2$^{R211L/R211L}$ x TAPP2$^{R218L/R218L}$ (TAPP KI) or p110d$^{D910A/D910A}$ (P110d) mice. Summary graph indicating the percent CD80+ or CD86+ from multiple mice per group is presented in Figure 1C.

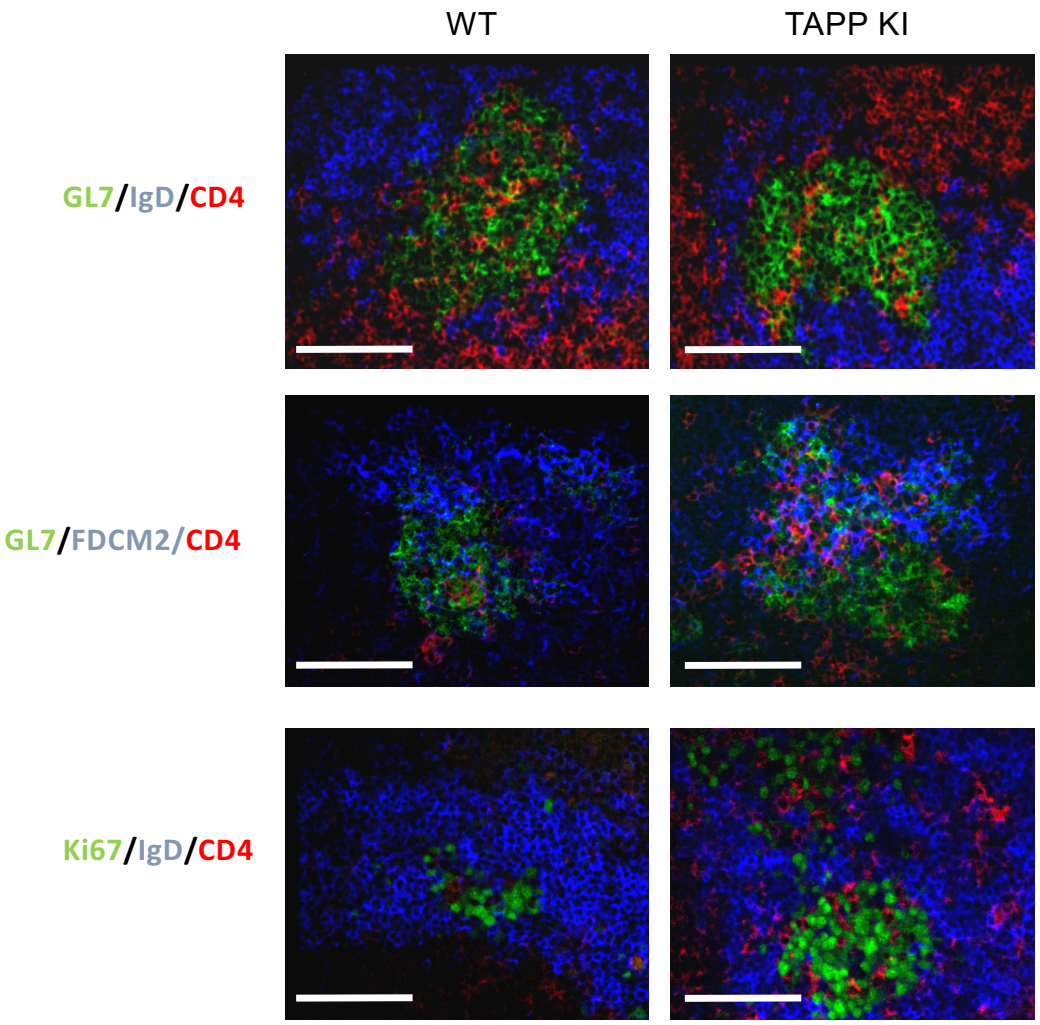


**Supplementary Figure 3. Additional microscopy images comparing wild-type and TAPP KI GC.**

Mice were immunized with NP-OVA precipitated in alum and spleens collected at day 8. Cryosections were stained for specific markers to detect GC B cells relative to IgD+ non-GCB cells and CD4+ T cells (top panels), FDC-M2+ follicular dendritic cells (middle panels), or to detect Ki67+ proliferating cells within IgD-negative GC (bottom panels) and. Scale bars, 100 μm.